

Commission No.: VII , No. of working group: 4

Wolfram M.C. Mueksch

Ardhi-Institute, University of Dar-es-Salaam, Tanzania

A verification trial of the coast morphology of sand embankment by surf waves from LANDSAT-imagery

Résumé

Des zones littorales de mangrove existent presque dans toutes les régions maritimes des pays équatoriaux. Ils forment la végétation des grandes deltas fluviales et des estuaires influencés par l'océan, causés par les sables et les sédimentations de vase.

L'estuaire de Wouri au Cameroun est une exemple typique. On peut observer les dépositions de sable et de vase totalement dans les images de LANDSAT sur la bande 4,5 et couleur false.

Les observations hydrographiques donnent une corrélation entre la propagation des vagues dans l'estuaire et les formes des dépositions.

Parcequ'il n'y a possible de réaliser une observation terrestre, ensemblée et détaillée dans le bay, qu'il est affecté par les tides, les recherches océanographiques ne sont qu'exécutées par des interprétations et des measurements sur les images de petite échelle.

L'expérience avec des dates structurales et spatiales de l'image avec la géométrie de la dynamique de propagation des vagues présente quelques interrelations quantitatives valables en l'espace d'une certaine tolérance. Néanmoins il existe des autres sources discrètes, causées par les tides, du vent, de l'influence saisonale, des turbulances, qu'elles trouvent leur limites de solution quantitative dans les grandes costes de l'observation et circonstances difficiles en measurement terrestre.

1. Geomorphological description of the delta and estuary structure of Wouri river

The coastal regions of african equatorial latitudes between 0° and 5° north (Gulf of Guinea) are highly characterized by mangrove swamps lying in the deltas and estuaries of large sediment transporting rain forest streams (Sanaga, Wouri, Mungo, Akpayafe) affected by the tides and the so called "Kalema" coming from the "Roaring Forties" in the Southern Atlantic.

The streams and rivers are originating in the mountainous areas and therefore show a lot of rapids with high velocity and transport energy.

The mangrove deltas and estuaries have surfaces often more than 500-1000 qkm with the highest elevation of 1 to 3m above sea level.

The meandering creeks or tidal channels is the characteristic pattern and radar images show a typical bright texture.

The estuary consists of a lot of larger creeks which give the typical tree structure and divide the borders into irregular shapes from where the creeks are starting. The mean depth is about 20m in the main creeks and the bay, ranging up to 20km from the oceanic coast from where the depth is slowly increasing.

The bottom of the estuary is changing by duning processes. The sand and slime deposits lie in the zones of shallow water starting around a depth of 5-10m. The embankments show a typical semi-ellipsed form of some kilometers in diameter from which the influence of the tides, the soft surf waves, lesser the breakers and other factors can be concluded.

The complete estuary structure and the oceanic influence is quite different from those of the Guinea-Bissau-Bay, where the sand deposits are diffusely scattered (LANDSAT scene No. E-30357-10411-5).

2. The ground observations

As it is the rule for remotely sensed data interpretations that they have to be verified by ground truth, the same has to be done in the case of wave studies.

While the theory of waves is well known since long each coast form shows its special wave influence.

During hydrographic surveys by the students of Survey School, Buea/Cameroon during 1977 the phenomena could be observed which formed the base of the interpretations.

The evident phenomenon is the tide variation seen at the mangrove roots. Parts of the sand and slime embankments are therefore over and under water during the tidal variations. The LANDSAT-scene shows the situation during the ebb.

When the flood is starting abruptly within a short time the typical surf wave curves are propagating against the shores and change the sediment level. The water level is raising in the creeks and the sand and slime is transported to the shore and the mouths of the creeks.

During the ebb the backstream transports the sediments into the sea, just at those positions of the rims where the flood before was discharging the material.

A typical cross section is developing changing permanently by deposition and denudation. Similar observation were made in (3,15).

This leads to the conclusion that the borders of the sediment surfaces are similar to the curves caused by the refraction of waves against the shore.

3. Short outlines of the surf wave theory

The application of the surf waves follows the theory, developed by the Russian oceanograph W.W.Schulejekin, who proved it by observations on the sea and in a storm basin

and published it in 1956(2).

The theory is starting with the refraction index $n=c_{\infty}/c$, where c_{∞} is the phase velocity of waves in a sea of unlimited depth.

Regarding the period of waves T and the wave length λ in shallow water one comes from the formula $\lambda_{\infty} = c_{\infty} \cdot T$ and the well known relation for the phase velocity in shallow water of a trochoidal wave:

$$c^2 = \frac{g\lambda}{2\pi} \operatorname{th} 2\pi \frac{H}{\lambda}$$

to the relative depth which is expressed by: $\mathcal{Y}_1 = H/T^2$.

With this formulas a diagram of the interrelation between n and \mathcal{Y}_1 can be derived and is represented by the hyperbolic approximation formula $n=1+m/\mathcal{Y}_1$ with the parameter $m=0.05$.

Applying the refraction law of Astronomy the form for a wave ray is: $n \cdot \sin \varphi = n_0 \cdot \sin \varphi_0 = n_0 \cdot \sin \beta_0 = \mathcal{C}$, in which φ is the general refraction angle against the normal axis of the shore.

Following the theory of light rays one comes to an expression of:

$$\frac{dy}{dx} = \sqrt{\left(\frac{n}{\mathcal{C}}\right)^2 - 1}$$

Regarding that the depth is increasing by a linear function the formulas given (in the tables at the end) are valid. Although the integral is simple it can only be solved by graphical integration.

For the practical evaluation the formula of the current refraction angle β_0 is important which is:

$$\sin \beta_0 = \frac{H_0 \sin \beta_1}{H_0 + mT^2}$$

where $\sin \beta_1$ is the direction angle against the normal axis to the shore in the starting zone of wave propagation. The same form of refraction theory can be applied in the inverse case caused by land wind.

$\lambda = 5.12 T^2$ is an empiric formula related from ground observations(15) from which the wave length can be derived.

4. Measurement of LANDSAT-imagery, data transformations and application of surf wave theory

The data collection was carried out by point wise coordinate measurements of the deposit shapes on a false colour frame. An older model of coordinate measuring machine of the Astronomical Institute of Bonn University was used which produced a semi-automatic output with a sensitivity of $1 \mu\text{m}$.

The definitions of the points had to be done during the measuring process and was difficult because of the low resolution of the borders of the deposits by the pixels and a nonvariable magnification of the eyepiece.

To minimize the errors and eliminate movements of the

frame, sharp defined points were measured at the beginning and at the end of the measurement which served as control points of the topographical map 1:50 000 of IGN/Cameroon. The final error of the measurement was $\pm 16 \mu\text{m}$ in x and $\pm 24 \mu\text{m}$ in y-direction. For the analysis the coordinates were transformed by a similarity transformation (Helmert) and then translated and rotated into local systems with x-axis parallel to the shore and positive y-axis against the sea.

The formulas described were applied by a stepwise approximation and adjustment procedure proving relations of wave periods ranging from 1-10sec. and 10° to 80° of the direction angle with an interval of 10° .

The average slope gradient was around 0.014 according to the ground observations.

5. Results and interpretations

A simulation program runned on the IBM 370/168 of RHRZ Bonn University Computer Center gave out a statistic of the mean error in meters between the theoretical model and the geometry of deposit shapes influenced by various direction angles β_1 of the surf waves against the shore normal axis.

The second test was made in respect to the decreasing refraction angle β_0 during the wave propagation compared with the respective angle computed from the deposit curve coordinates for the different wave periods within the tolerances $\Delta\beta < 10^\circ, 5^\circ, 2^\circ, 1^\circ$. The output was the applicable direction angle β_1 , the refraction angle β_0 for various periods, the actual angle β_1 from the coordinates and the period itself.

Correlations with the numbers of digitized points and the numbers of direction angles β_1 were eliminated by stepwise reductions of the numbers of border points and calculating the differences of the simulations of $\Delta\beta < 5^\circ, 2^\circ, 1^\circ$ against the one of $\Delta\beta < 10^\circ$ instead of absolute values.

The reactions of the output datas were the same as in the simulations with the complete data sets. Therefore the following results given are statistically valid for all manipulations carried out:

- The wave directions of $20-30^\circ$ against the normal axis are the most frequent ones (the portion is 40%). The rest of the 60% distributes on the other directions ranging from $10-80^\circ$ (Fig.1).
- With the increasing directions from 40° upward the deviations of the deposit borders from the theoretical model are becoming smaller. This leads to the conclusion that the waves of these directions are "grinding off" permanently and form certain parts of the rims.
- The stronger the curvature of the deposits are, the smaller the direction angles are, i.e. $20-30^\circ$. It supports the fact that the flood has a greater influence than

the ebbstream in the Wouri-estuary.

- The mean deviation of all deposit curves of the theoretical model was $360 \pm 170\text{m}$ which is around 10% of the average length and 20% of the average width of the deposit surfaces.
- Accumulations of errors are found between 100 and 300 and 400 to 500m with the relation that a ratio of shore length to width of 2:1 corresponds with the lower error and the reciprocal ratio is related to the higher error. The conclusion is that the waves nearer to the shore have greater influence on the deposits of the first type, because the rays are stronger curved in the shallow water (Fig.2).

A comparison of the theoretically computed angles β_0 with those β_i simulated by the deposit coordinates gave certain aspects of the dynamics of wave propagation within the range of position errors:

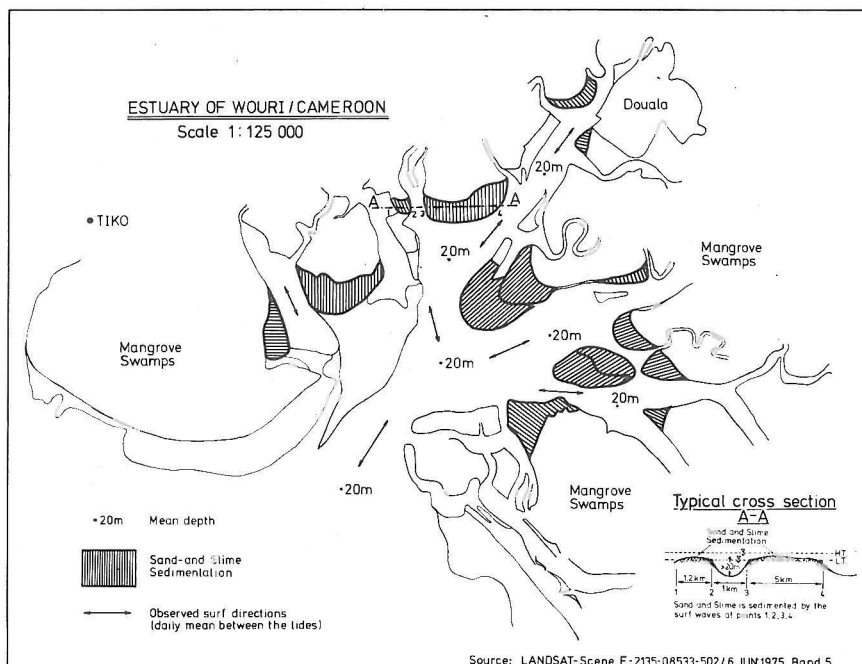
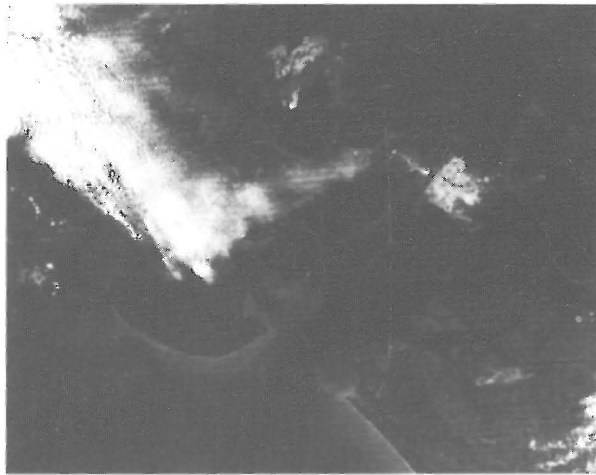
- For the angles 20° and 30° the change of periods from 1 to 7sec. is slow; the periods 8 to 10sec. are changing faster against the shore. The higher the parallelity of wave propagation to the shoreline is, the faster the shorter periods are disappearing in the sea (the obvious base phenomenon mentioned above).
- This fact will also be supported by the graph of the numbers of one and the same period on the deposit curves for all tolerances of $\Delta\beta$ simulated. The number is decreasing rapidly from 5 to 10sec. This process is stopping as soon as the angle tolerances are decreasing. At the tolerance of $\Delta\beta < 1^\circ$ all periods are equally distributed on the deposit curves (Fig.4).
- An analysis of the trend numbers of the periods being mostly negative are showing a declining tendency of 84% to longer periods, so that these wave types are finally coming to the shore (Fig.5-8).
- Equally curved deposit shapes present the largest numbers of each period type for all direction angles and tolerances.
- This is also valid as soon as the curvature is changing uniformly to increasing or decreasing gradients.
- Further tests for the case $\Delta\beta < 1^\circ$ stated the existence of an only weak correlation of $r=0.21$ between the true differences $\Delta\beta$ and the periods.

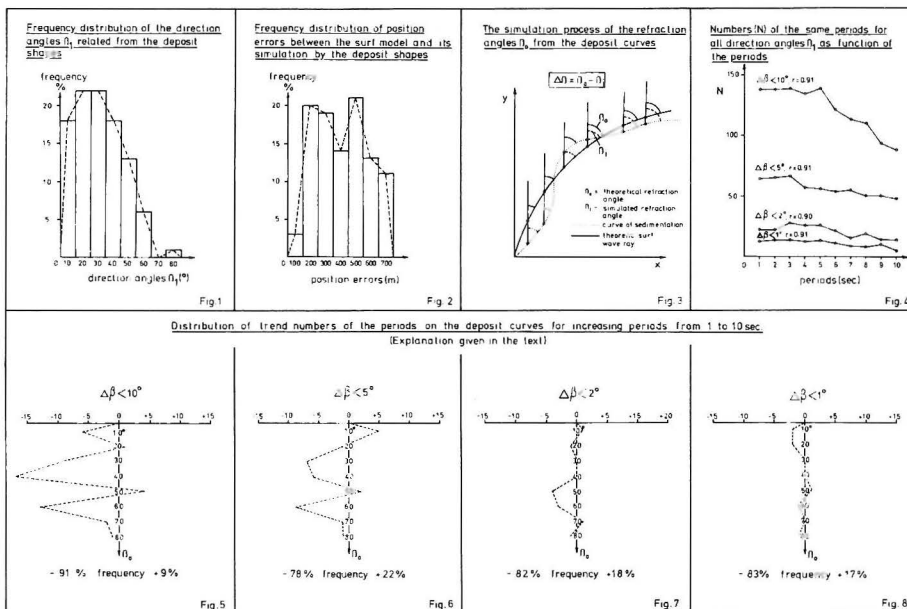
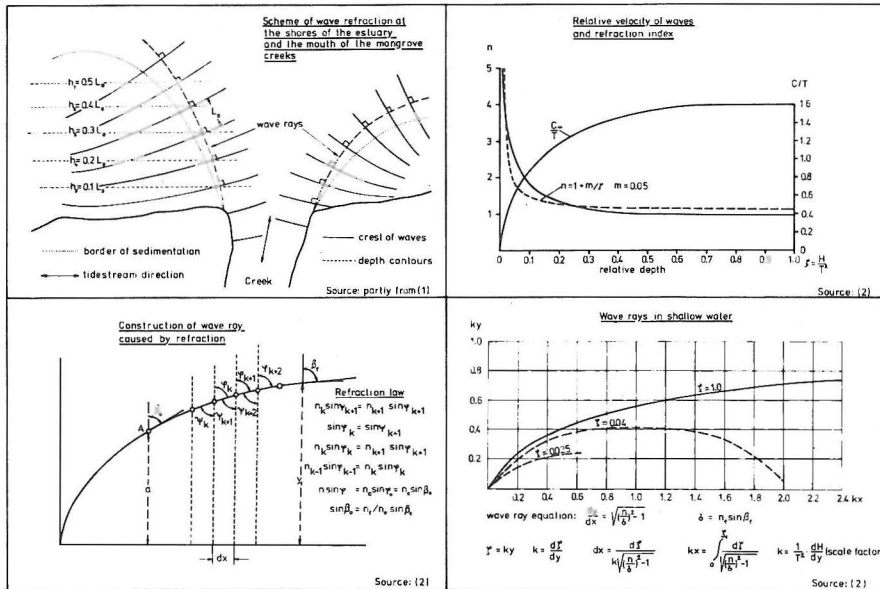
6. Final conclusion

The quantitative and empiric treatment of the surf wave dynamics by simulation with the deposit shapes give indeed an "amazing" significance. It would be to far interpreted that the sedimentation process is caused mainly by soft surf waves. Other factors as wind, ebbstream, turbulences, the

well known phenomenon of the breakers and the fluvial processes play an additional important role which must be taken in consideration for complete quantitative statements.

The trial with this simulation shows that satellite imagery indeed offers observations and interpretations of quantitative complex dynamic coast and oceanic submarine processes within a certain validity which in an other way is only obtainable by difficulties and high, less justified costs.





Calculation of position errors

ROTATION ANGLE		TRANSFORMED COORDINATES	
β_1	β_2	COORD	YCOORD
100	42024.96	3.00	
100	360	3.00	
100	10072.20	1072.65	
104	3672.86	742.75	
108	1074.73	742.75	
108	1491.75	1074.67	
107	10002.63	1074.66	
100	2074.66	1711.25	
100	2074.66	1711.25	

Simulation of refraction angles

ROTATION ANGLE		TRANSFORMED COORDINATES	
β_1	β_2	COORD	YCOORD
100	42024.96	3.00	
100	360	3.00	
100	10072.20	1072.65	
104	3672.86	742.75	
108	1074.73	742.75	
108	1491.75	1074.67	
107	10002.63	1074.66	
100	2074.66	1711.25	
100	2074.66	1711.25	

ROTATION ANGLE		TRANSFORMED COORDINATES	
β_1	β_2	COORD	YCOORD
100	42024.96	3.00	
100	360	3.00	
100	10072.20	1072.65	
104	3672.86	742.75	
108	1074.73	742.75	
108	1491.75	1074.67	
107	10002.63	1074.66	
100	2074.66	1711.25	
100	2074.66	1711.25	

ROTATION ANGLE		TRANSFORMED COORDINATES	
β_1	β_2	COORD	YCOORD
100	42024.96	3.00	
100	360	3.00	
100	10072.20	1072.65	
104	3672.86	742.75	
108	1074.73	742.75	
108	1491.75	1074.67	
107	10002.63	1074.66	
100	2074.66	1711.25	
100	2074.66	1711.25	

Literature

- (1) G. Dietrich, Allgemeine Meereskunde, Berlin 1965
- (2) W. W. Schulejkin, Theorie der Meereswellen, Berlin 1960
- (3) Chuchlaine A. M. King, Techniques in Geomorphology, London 1966
- (4) J. C. Doornkamp, C. A. M. King, Numerical Analysis in Geomorphology, London 1970
- (5) R. J. Chorley, Introduction to fluvial Processes, London 1969
- (6) J. A. Ngwa, An Outline Geography of the Federal Republic of Cameroon, London 1967
- (7) Hagget-Chorley, Network Analysis in Geography, London 1969
- (8) F. F. Sabins, Remote Sensing, Principles and Interpretations, San Francisco 1968
- (9) H. Wolf, Ausgleichungsrechnung nach der Methode der kleinsten Quadrate, Bonn 1968
- (10) W. Mueksch, Die Verwendbarkeit von LANDSAT-Bildern bei landwirtschaftlichen Planungen in tropischen Sumpf- und Regenwaldzonen, Bildmessung und Luftbildwesen, BuL, 6/1979
- (11) Leopold and Langbein, River Meanders, Scientific American, 1966
- (12) Leopold, Wolman, Miller, Fluvial Processes in Geomorphology, San Francisco 1964
- (13) H. G. Gierloff-Emden, Manual of interpretation of orbital remote sensing satellite photography and imagery for coastal and offshore environmental features (including lagoons, estuaries and bays, Mün chener Geogr. Abhandlungen, Institut für Geographie, München, 1976, publ. by Intergovernmental Oceanographic Commission
- (14) C. A. M. King, Beaches and Coasts, London
- (15) Davies, J. L., Wave refraction and evolution of shoreline curves, Geogr. Studies, 5/1959